© 2020. Published by The Company of Biologists Ltd | Journal of Cell Science (2020) 133, jcs247312. doi:10.1242/jcs.247312

RESEARCH ARTICLE

RGS4 controls secretion of von Willebrand factor to the subendothelial matrix

Francesca Patella and Daniel F. Cutler*

ABSTRACT

The haemostatic protein von Willebrand factor (VWF) exists in plasma and subendothelial pools. The plasma pools are secreted from endothelial storage granules, Weibel–Palade bodies (WPBs), by basal secretion with a contribution from agonist-stimulated secretion, and the subendothelial pool is secreted into the subendothelial matrix by a constitutive pathway not involving WPBs. We set out to determine whether the constitutive release of subendothelial VWF is actually regulated and, if so, what functional consequences this might have. Constitutive VWF secretion can be increased by a range of factors, including changes in VWF expression, levels of TNF and other environmental cues. An RNA-seq analysis revealed that expression of regulator of G protein signalling 4 (RGS4) was reduced in endothelial cells (HUVECs) grown under these conditions. siRNA RGS4 treatment of HUVECs increased constitutive basolateral secretion of VWF, probably by affecting the anterograde secretory pathway. In a simple model of endothelial damage, we show that RGS4-silenced cells increased platelet recruitment onto the subendothelial matrix under flow. These results show that changes in RGS4 expression alter levels of subendothelial VWF, affecting platelet recruitment. This introduces a novel control over VWF function.

KEY WORDS: Weibel–Palade bodies, von Willebrand Factor, Extracellular matrix, RGS4, Constitutive secretion

INTRODUCTION

Endothelial von Willebrand factor (VWF) plays several roles in haemostasis. This is reflected not only in its central role as a mechanosensitive-binding platform for platelets, but also in its presence in three secreted pools. VWF stored in Weibel–Palade bodies (WPBs) can be released either by localised agonist-stimulated exocytosis, to provide transient VWF strings on the endothelial surface that initiate primary haemostasis, or by general basal secretion, to provide the large pool of circulating plasma VWF (Lopes da Silva and Cutler, 2016). The third VWF pool is released by constitutive secretion into the subendothelial matrix, where it presumably acts in platelet recruitment following exposure by injury.

This latter pool of VWF is the least well understood. We previously reported that it comprises very poorly multimerised VWF, that is not stored in WPBs but secreted by a constitutive pathway targeted to the subendothelial space, where it likely binds to the extracellular matrix (Lopes da Silva and Cutler, 2016). Both the regulation of this pathway and a direct analysis of the function of this VWF after delivery remain elusive. Here, we used RNA-seq to analyse cells treated with different regimes that increased constitutive VWF secretion, allowing the identification of regulator of G protein signalling 4 (RGS4) as a commonly downregulated mRNA and as a candidate modulator of this constitutive pathway. RGS4 is known to act both as a GTPase-activating protein (GAP) (Watson et al., 1996; Berman et al., 1996) and can also bind to β′COP (also known as COPB2) (Sullivan et al., 2000), a component of the machinery underpinning the retrograde secretory pathway. Both of these functions could potentially modulate a constitutive secretory pathway. We used RGS4 siRNA to show that this protein does indeed regulate constitutive secretion of VWF to the subendothelial matrix, and developed an assay mimicking endothelial damage, by stripping endothelial cells from their extracellular matrix, to determine the effects on platelet recruitment under flow of changing levels of RGS4. We conclude that altering the amount of constitutively secreted VWF into the subendothelial space by decreasing RGS4 levels in endothelial cells can indeed alter platelet recruitment to an exposed subendothelial surface in a simplified model of injury.

RESULTS

Identification of a candidate for control of constitutive VWF secretion in endothelial cells

To identify regulators of constitutive VWF secretion, we challenged human umbilical vein endothelial cells (HUVECs) with conditions known to increase unregulated (i.e. basal plus constitutive) VWF secretion. We used brefeldin A (BFA) treatment to distinguish between basal and constitutive secretion (Giblin et al., 2008; Lopes da Silva and Cutler, 2016); BFA selectively blocks constitutive secretion by disrupting endoplasmic reticulum (ER) to Golgi transport, thus preventing exit of newly synthesized material from the ER without affecting secretion from post-Golgi organelles, such as WPBs (including basal secretion of VWF) (Fig. 1A). The conditions that we tested, shown in the referenced literature to increase unregulated VWF secretion, were: (1) VWF knockdown (KD) by siRNA (si-VWF) (Ferraro et al., 2014); (2) nocodazole treatment (Ferraro et al., 2014); (3) TNF treatment (Bernardo et al., 2004; van der Poll et al., 1992); (4) MyRIP KD (si-MyRIP) (Bierings et al., 2012; Nightingale et al., 2009); (5) GRK2 KD (si-GRK2) (Stevenson et al., 2014); and (6) EBM2 medium (from our unpublished observations). We also used AP1 KD as a positive control for the maximum possible constitutive output that could be obtained by switching all VWF secretion to constitutive [AP1 is essential for WPB formation, and once ablated, the major WVF secretory pathways (basal and agonist-stimulated) are redirected towards the constitutive pathway (Lui-Roberts et al., 2005; Lopes da Silva and Cutler, 2016)]. These experiments

MRC Laboratory for Molecular Cell Biology, University College London, London WC1E 6BT, UK.

*Author for correspondence (d.cutler@ucl.ac.uk)

D.F.C., 0000-0002-4288-7530

Handling Editor: David Stephens
Received 7 April 2020; Accepted 11 June 2020

Journal of Cell Science (2020) 133, jcs247312. doi:10.1242/jcs.247312

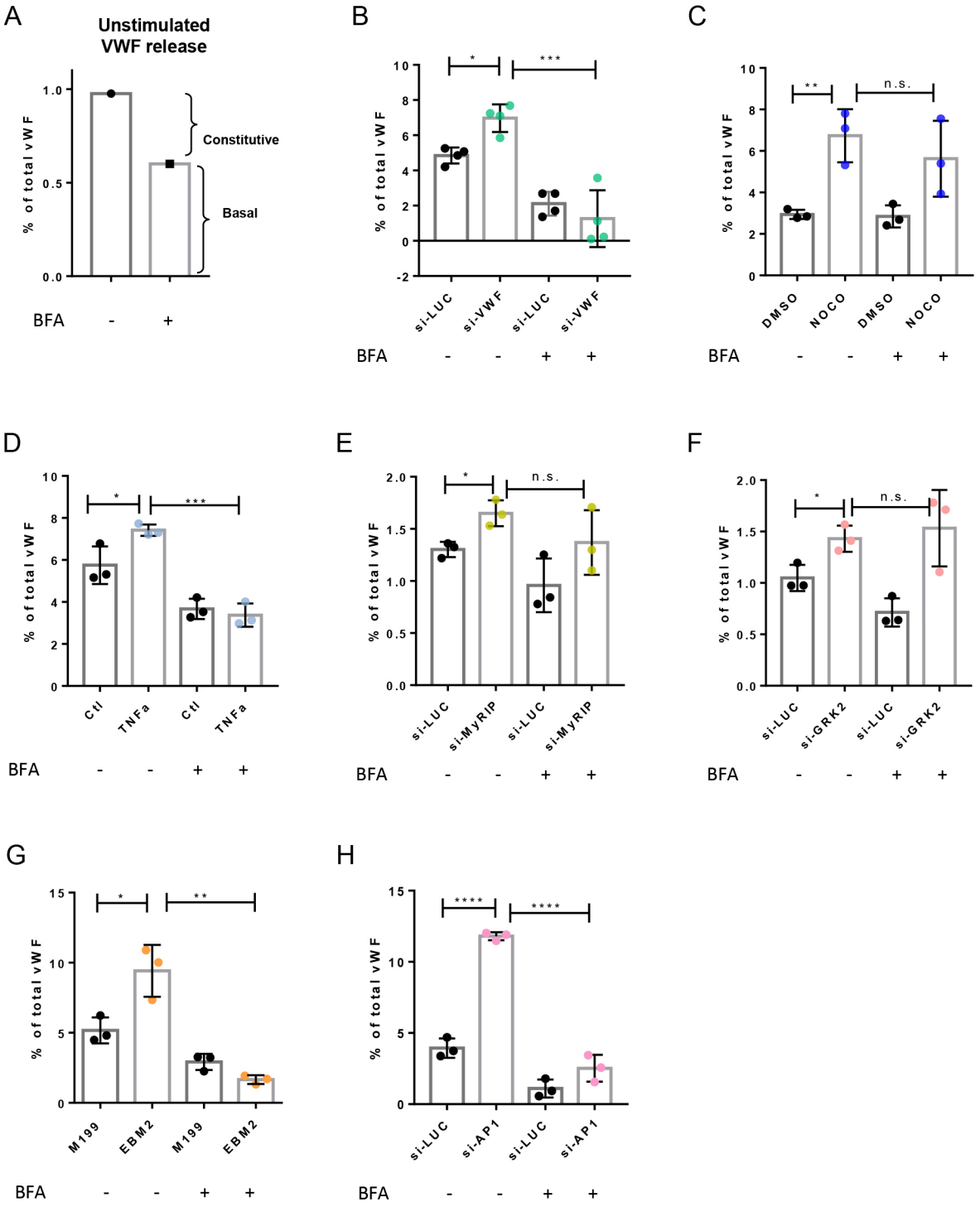

Fig. 1. Conditions increasing constitutive VWF secretion in HUVECs. (A) To measure and distinguish between basal and constitutive VWF secretion we deployed brefeldin A (BFA), a drug able to block constitutive secretion without affecting the release of pre-formed VWF-containing organelles (WPBs) via basal release. (B–H) HUVECs were challenged with the indicated conditions known to increase unstimulated VWF secretion: VWF KD (si-VWF) (B), nocodazole (C), TNF (D), MyRIP KD (si-MyRIP) (E), GRK2 KD (si-GRK2) (F), EBM2 medium (G), AP1 KD (si-AP1) (H). The amount of secreted VWF (in the absence of any stimulant) was measured by ELISA and plotted as a percentage of the total VWF in cells. Conditions shown in A, C and F were further investigated because they induced an increase in constitutive secretion versus basal secretion, since that increase was blocked by BFA. In B–H, a representative experiment with mean±s.d. of technical replicates is shown from n=3 independent experiments. *$P\leq0.05$; **$P\leq0.01$; ***$P\leq0.001$; ****$P\leq0.0001$; n.s., not significant (Student's t-test).

(Fig. 1B–H) showed that – besides AP1 depletion – suppressing VWF levels, treating with TNF, and growth in EBM2 medium all increased constitutive VWF release, while the other treatments only affected basal release.

To identify common factors among the three treatments, we used an RNA-seq approach (Tables S1–S3). No genes were found to be commonly upregulated in the three conditions, but two genes – those encoding RGS4 and Gap junction protein α5 (GJA5) – were

Journal of Cell Science (2020) 133, jcs247312. doi:10.1242/jcs.247312

downregulated in the si-VWF, TNF and EBM2 conditions (Fig. 2A, B). Since RGS4 is a cytosolic protein that has already been shown to be involved in negatively regulating agonist/receptor-stimulated secretion of insulin (Ruiz de Azua et al., 2010) and catecholamines (Iankova et al., 2008), we further investigated its role in constitutive VWF secretion. We first confirmed by quantitative (q)PCR that *RGS4* mRNA was downregulated in all three conditions (Fig. 2C), but not when constitutive secretion was not affected (i.e. in nocodazole treatment, MyRIP KD, GRK2 KD and AP1 KD) (Fig. 2D). Interestingly, while AP1 KD does increase constitutive secretion of VWF, it does not decrease *RGS4* expression, whereas when *RGS4* expression is decreased in TNF, EBM2, VWF KD conditions, we did not find changes in AP1 expression (Fig. 2D; Tables S1–S3), suggesting that AP1 and RGS4 act through different mechanisms. Since we were not able to measure RGS4 by immunoblotting using commercial antibodies, we used an indirect approach to check whether the phenotype we observed upon decreased *RGS4* mRNA expression with the different treatments was due to a consequent diminished amount of RGS4 protein. We treated the cells with a NO donor (S-nitroso-L-cysteine; CysNO), known to induce RGS4 proteasomal degradation (Jaba et al., 2013; Hu et al., 2005), and then measured VWF secretion compared to control cysteine (Ctl_cys). We noticed an increase in unstimulated VWF secretion in cells treated with CysNO (Fig. 2E), and this prompted us to conclude that the treatments causing increased unstimulated VWF secretion also affected general RGS4 expression, not just its mRNA.

RGS4 KD increases constitutive VWF secretion from the basolateral side of HUVECs

To verify that the decreased expression of RGS4 was directly responsible for increasing constitutive VWF secretion we used an siRNA approach (Fig. 3A). si-RGS4 affected neither the length distribution nor the number of WPBs (Fig. 3B,C), but it increased constitutive VWF secretion ∼2-fold (Fig. 3D). To analyse any effect on the polarity of secretion, we seeded the HUVECs in Transwell inserts and collected the medium from the top well (releasate from the apical side) and the bottom well (releasate from the basolateral side) (Fig. 3E). This revealed that the increase in VWF secretion upon si-RGS4 was mostly from the basolateral surface of the cells and was indeed constitutive, since it was blocked by BFA (Fig. 3F). To test whether this effect of RGS4 KD was specific to VWF secretion, we transfected the cells with a lumGFP construct (Blum et al., 2000; Knipe et al., 2010), a cargo known to be secreted constitutively in HUVECs but in a non-polarised way (Lopes da Silva and Cutler, 2016). RGS4 did not affect either the amount or polarity of lumGFP secretion, suggesting that its action is at least partly specific to VWF (Fig. 3G). These data indicate that RGS4 negatively regulates the basolateral secretion of VWF from endothelial cells.

The β′-COP-binding activity of RGS4 is responsible for constitutive VWF secretion

RGS4 is known to have at least two activities: to act as a GAP for heterotrimeric G proteins and to bind β′-COP, a subunit of the COPI

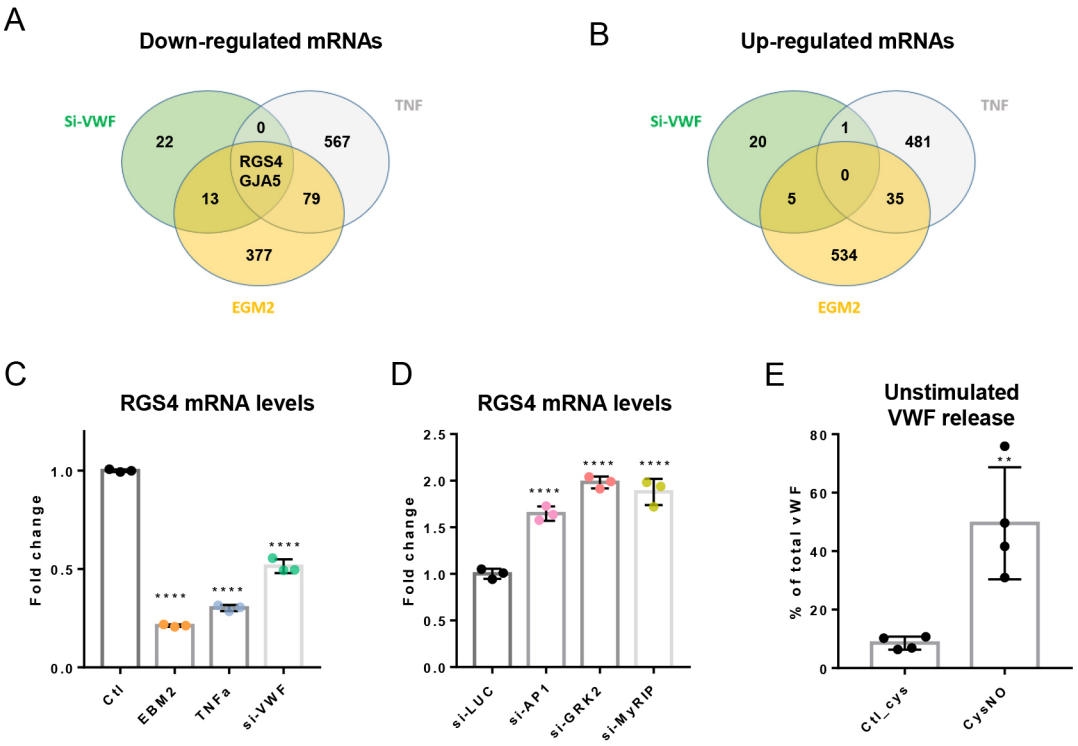

Fig. 2. Identification of a regulator of constitutive VWF secretion in HUVECs. A comparison of the transcriptome (made by RNA-seq) of the previously selected conditions (si-VWF, EBM2 and TNF) relative to their respective controls enabled us to identify a putative regulator of constitutive VWF secretion. The Venn diagrams show the number of downregulated (A) and upregulated transcripts (B). *RGS4* and *GJA5* were the only transcripts found to be significantly regulated (underexpressed) upon all three treatments (A,C), while in the other treatments where constitutive secretion was not affected (GRK2 KD and MyRIP KD) or in AP1 KD (an independent regulator of constitutive secretion), *RGS4* mRNA was upregulated (D), as measured by qPCR. In C and D, a representative experiment with mean±s.d. of technical replicates is shown from n=2 independent experiments. ****P<0.0001 (one-way ANOVA with Dunnett's multiple comparisons test). (E) A NO donor (CysNO), which affects RGS4 at the protein level, triggering its degradation, increases unstimulated VWF secretion compared to the Cys control. A representative experiment with mean±s.d. of technical replicates is shown from n=3 independent experiments. **P≤0.01 (Student's t-test).

Journal of Cell Science (2020) 133, jcs247312. doi:10.1242/jcs.247312

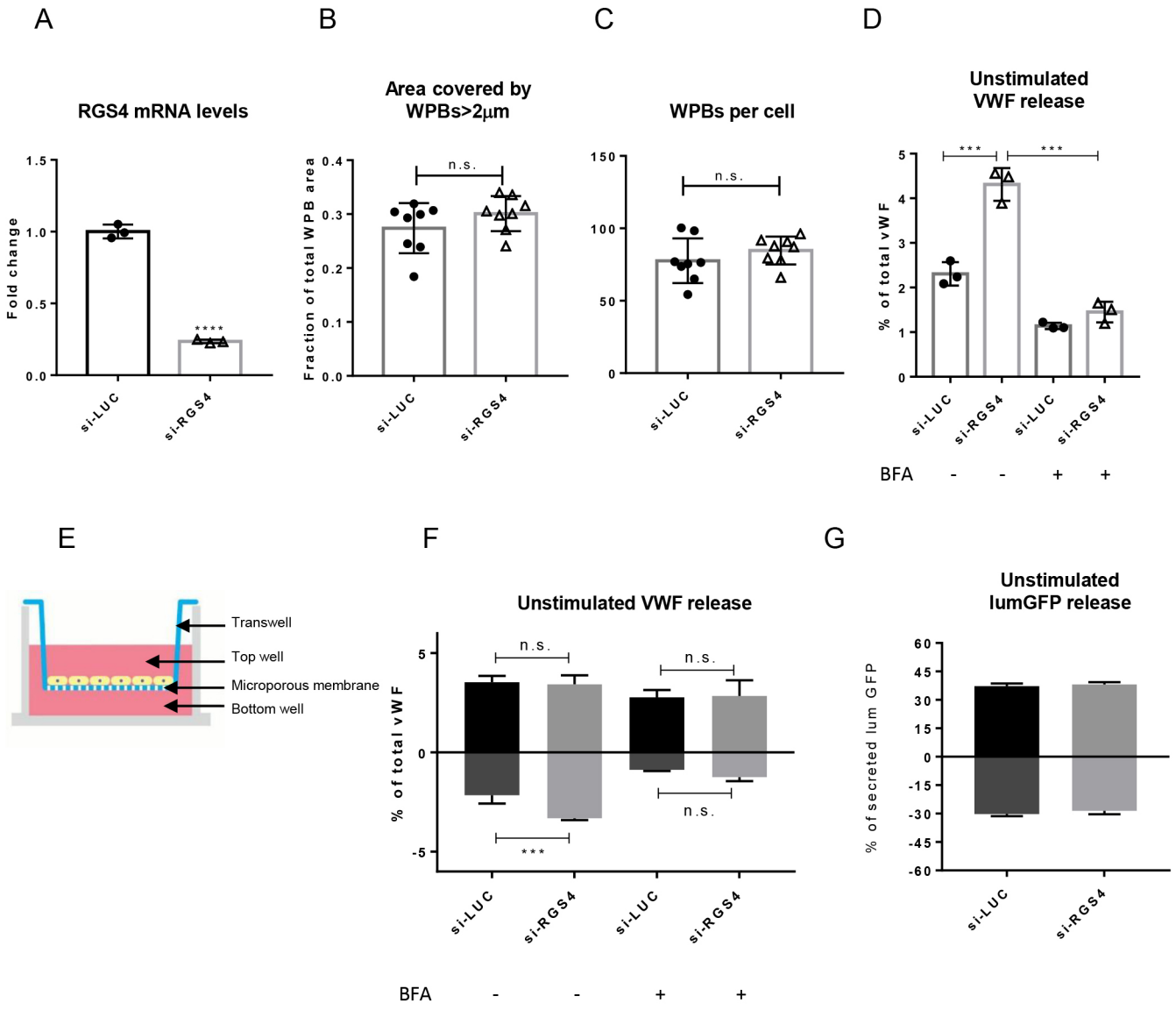

Fig. 3. RGS4 KD increases constitutive VWF secretion from the basolateral side of HUVECs. (A) We successfully reduced *RGS4* mRNA in HUVECs with siRNAs. A representative experiment with mean±s.d. of technical replicates is shown from n=4 independent experiments. ****P<0.0001 (Student's t-test). (B–D) As assessed through high-throughput imaging experiments, we did not observe changes in the length of WPBs (the area covered by the longer WPBs, those greater than 2 µm, is used as a proxy for length) in the RGS4 KD cells (B), or in the number of WPBs per cell (C), n=8 wells (for each well the mean of nine fields of view were analysed). n.s, not significant (Student's t-test). We did measure, by secretion assay followed by ELISA, an increase in constitutive VWF secretion (D). The plot shows means±s.d. of a representative experiment from n=3 independent experiments. ***P≤0.001 (Student's t-test). (E–G) Plating cells in Transwell inserts enabled us to better dissect the route of the increased constitutive VWF secretion (as assessed by comparing with and without BFA) upon RGS4 KD (F), which was mainly released towards the basolateral side of the HUVECs. When using a construct expressing a constitutively secreted protein (lumGFP), we did not measure changes in its secretion upon RGS4 KD (G). In F,G a representative experiment with mean±s.d. of technical replicates is shown from n=3 independent experiments. ***P≤0.001; n.s., not significant (Student's t-test).

coatomer complex essential to retrograde transport from the trans-Golgi network to the cis-Golgi network and ER (Sullivan et al., 2000). In principle, either activity could affect constitutive secretion; heterotrimeric G-proteins are active at the Golgi (Giannotta et al., 2012; Cancino et al., 2014), and we have recently shown that modulating retrograde trafficking that is dependent on COP1-coated vesicle transport can affect exit from both the ER and from the TGN (Lopes-da-Silva et al., 2019). To test whether RGS4 depletion affects G-protein signalling or binding to β′-COP, we overexpressed (OE) a GAP-dead RGS4 mutant (N128A) (Fig. 4A), or an RGS4 mutant with a deleted (delta131–205) (Fig. 4B) or mutated (K100E) (Fig. 4C) binding site for β′-COP. When over-expressed in identical circumstances, the GAP-dead construct had no effect on unstimulated VWF secretion, but the constructs unable to bind β′-COP were able to replicate the phenotype observed upon RGS4 depletion. These experiments suggest that RGS4 may indeed act as an indirect brake on constitutive secretion of VWF from HUVECs by interfering with the retrograde trafficking pathway that recycles machinery for re-use by the anterograde constitutive pathway.

The functional activity of VWF delivered to the subendothelial matrix is regulated by RGS4

Our data provide evidence that RGS4 controls constitutive basolateral secretion of VWF. Since this pool of VWF is released

Journal of Cell Science (2020) 133, jcs247312. doi:10.1242/jcs.247312

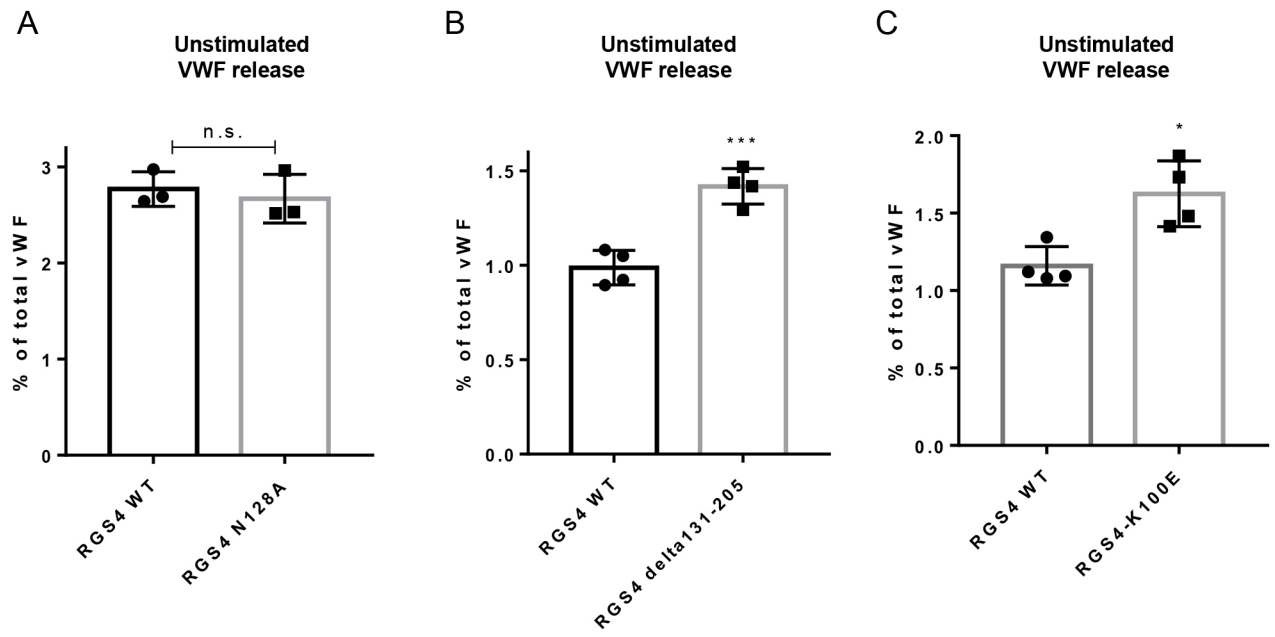

Fig. 4. The β′-COP-binding activity of RGS4 is responsible for constitutive VWF secretion. To understand which of the two known functions of RGS4 is responsible for controlling constitutive VWF secretion, we expressed and compared the effects of mutated and wt RGS4 constructs. Expressing a GAP dead mutant (N128A) does not change the amount of unstimulated VWF secretion (A), whereas expressing a construct lacking the binding site for β′-COP (delta131–205) or mutated in the β′-COP binding activity (K100E) results in an increase in unstimulated VWF secretion (B,C). A representative experiment with mean±s.d. of technical replicates is shown from *n*=3 independent experiments. **P*≤0.05; ****P*≤0.001; n.s., not significant (Student's *t*-test).

into the subendothelial matrix and is only in contact with circulating blood when there is an injury compromising the endothelial layer, we sought to determine the functional significance of this poorly characterised pool of VWF. We therefore designed an experiment to mimic injury that would result in exposure of the subendothelial matrix to platelets under flow. We plated si-RGS4 or control HUVECs in flow chambers, allowed them to grow to confluence, then removed the cells under flow, and passed whole blood or platelets over the exposed subendothelial matrix. After fixation and antibody labelling of VWF, we quantified, by means of immunofluorescence microscopy, both that RGS4 KD did lead to more VWF being present within the matrix (Fig. 5A), and that there was increased platelet recruitment (shown by the marker CD41), either from whole blood (Fig. 5B,C) or isolated platelets (Fig. 5D). Taken together, this suggests that by regulating secretion of VWF into the subendothelial space, RGS4 can potentially control the ability of an endothelium-denuded surface, such as an injured vessel wall to recruit platelets to the exposed matrix.

DISCUSSION

VWF is released from endothelial cells into three pools, of which that located within the subendothelial matrix has only recently been characterised. In this work, we show that the secretion of this pool of VWF is regulated, affecting the recruitment of platelets when exposed.

We have previously shown that not only is this pool of VWF targeted for release towards the subendothelial space, but is constitutively secreted (i.e. not stored within WPBs), and thus cannot undergo the complex biogenesis seen for the rest of VWF. It largely remains as dimers, not forming the ultra-large concatamers that are generated within the TGN/WPB (Lopes da Silva and Cutler, 2016). This subendothelial matrix pool is not only of much lower molecular mass, but also does not form the coils that support multimerization that is characteristic of lumenally secreted VWF. It is not likely to be stretched under flow to optimise its ability to recruit platelets, but rather may bind to elements, such as collagen, within the matrix, potentially even saturating available VWF-binding sites (although under our standard growth conditions, this seems not to be the case). Nevertheless, VWF bound to the extracellular matrix was shown to be able to bind to platelets under flow (Baruch et al., 1991; Stel et al., 1985; Sixma et al., 1987; Houdijk et al., 1986). Here, we have found that the constitutive release of VWF into this pool can be controlled by RGS4, a poorly characterised protein with two previously identified functions. Our experiments showed that this protein acts to modulate the constitutive secretion of VWF, likely via its ability to bind to β′-COP. β′-COP is essential for the formation of COP1 coats that support retrograde vesicular transport from the TGN all the way back to the ER. Interfering with retrograde transport, for example, by suppressing GBF1, which controls COP1 coat assembly by Arf1 and Arf4, also leads to modulation of VWF anterograde traffic (Lopes-da-Silva et al., 2019). In that previous study, we also reported dramatic effects on WPB formation at the TGN. Inhibiting retrograde traffic reduced recycling of components essential to anterograde trafficking, causing hold-ups at ER and TGN exit, the latter leading to the formation of giant WPBs. Here, we speculate that, by removing RGS4, we are promoting retrograde and anterograde trafficking, and hence also constitutive VWF trafficking, without significantly affecting WPB size.

Binding of RGS4 to β′-COP was previously shown to prevent COPI binding to purified Golgi membranes and to impair constitutive trafficking of aquaporin in LLC-PK1 cells (Sullivan et al., 2000). Consistent with this, we show that RGS4 depletion, or overexpression of RGS4 lacking the ability to bind β′-COP, caused an increase in constitutive VWF secretion to the subendothelial side of endothelial cells, arguably by removing the brake on β′-COP and promoting β′-COP function in retrograde/anterograde trafficking. How specific to VWF this mechanism might be remains to be

Journal of Cell Science (2020) 133, jcs247312. doi:10.1242/jcs.247312

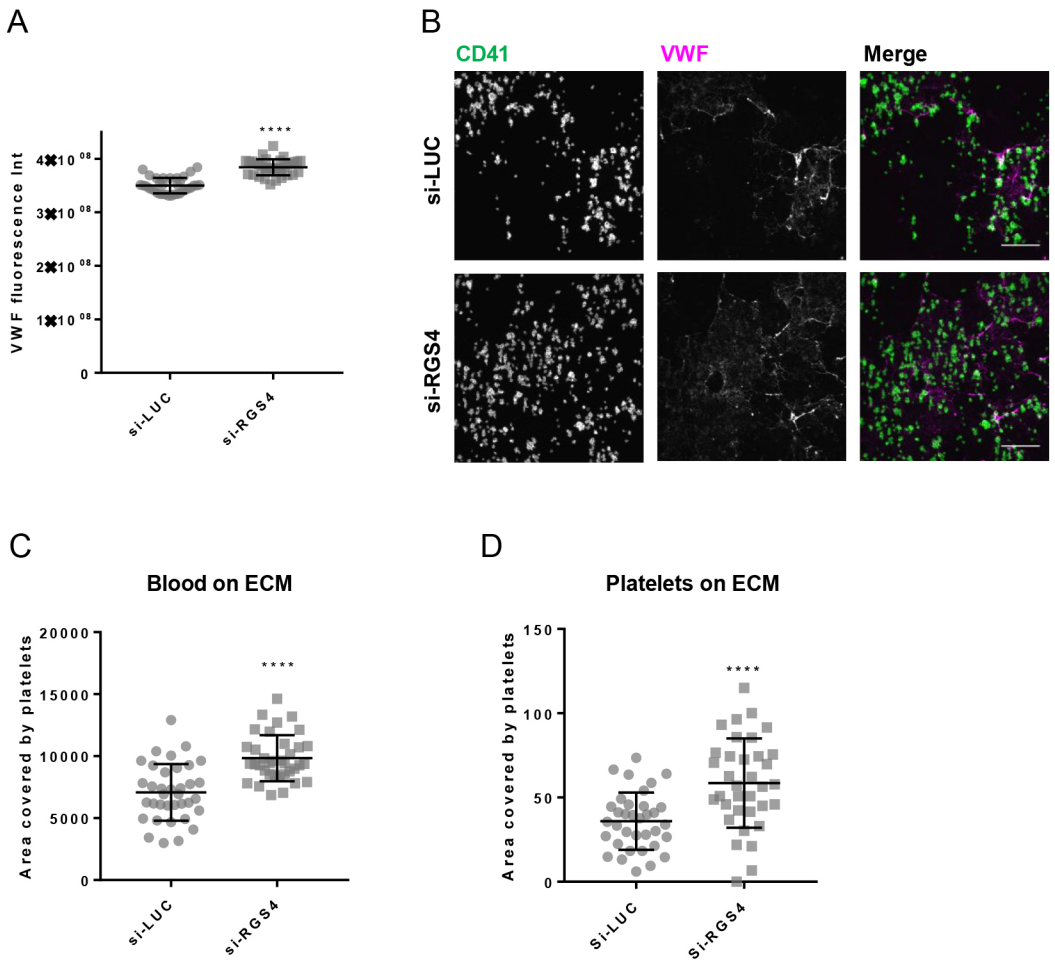

Fig. 5. Constitutive basolateral VWF secretion provides a functional pool of VWF in the subendothelial space. The removal of HUVECs exposed the subendothelial matrix and the VWF bound to it. Upon decellularisation, more VWF is bound to the extracellular matrix in RGS4 KD cells. (A) Scatter plots present mean±s.d. of a representative experiment from n=3 independent experiments. Each symbol is the VWF fluorescence intensity (integrated density) of a field of view. ****P<0.0001 (Student's t-test). (B) Confocal microscopy showing VWF (magenta) and platelets (green, CD41) after superfusion of the exposed subendothelial matrix with blood. Scale bars: 50 µm. We could see more platelets adherent in the RGS4 KD compared to control both when we superfused whole blood (B,C) and also when we superfused isolated platelets (D) over the decellularised matrix. In C,D a representative experiment with mean±s.d. is shown from n=3 independent experiments. Each symbol represents the area covered by platelets (n=35 fields of view). ****P<0.0001 (Student's t-test).

elucidated. Our experiments suggest that in HUVECs, RGS4 KD specifically increases constitutive VWF secretion, but more sensitive approaches (e.g. using proteomics) could be used to fully address this question.

Is this mechanism likely to be used for physiological control? One possible mechanism would involve nitrous oxide (NO), a promoter of a healthy, anti-atherogenic endothelial phenotype, which is also able to trigger the proteasomal degradation of RGS4 (Jaba et al., 2013; Hu et al., 2005). We speculate that when NO is induced, it will increase the secretion of VWF towards the subendothelial space, but not towards the vessel lumen into the plasma VWF pool. In this way, NO will not drive the formation of a plug that could become a thrombus, because the subendothelial VWF will only become exposed when damage has already occurred. The well-known anti-platelet actions of NO (Mellion et al., 1981; Radomski et al., 1990) can thus act in the lumen of the vessel without jeopardising a VWF-dependent haemostatic response to actual injuries that expose VWF in the subendothelial space.

This work focusses on the neglected constitutive pool of VWF that not only has a different mode of biosynthesis from the better understood WPB-associated pools, but is also differentially targeted for secretion to the subendothelial space, and at least in part is regulated by separate machinery, depending on RGS4. Further details of all the mechanisms involved in the control of this pool, whose secretion was previously believed to be uncontrolled (i.e. constitutive), plus the functional consequences of its regulation now clearly warrant future investigation.

MATERIALS AND METHODS

Cell culture

Human umbilical vein endothelial cells (HUVECs) pooled from multiple donors are from PromoCell and used within the fifth passage. Cells were cultured in M199 (Thermo Fisher Scientific, UK) or EBM2 (Promocell, Heidelberg, Germany) with 20% fetal bovine serum (Labtech, Heathfield, UK), 30 µg/ml endothelial cell growth supplement from bovine neural tissue (Sigma-Aldrich, UK) and 10 U/ml heparin.

Nocodazole (1 µg/ml) and TNF (50 ng/ml) were from Sigma-Aldrich, UK. Nocodazole and TNF treatment were for 16 and 24 h, respectively.

siRNA transfection

We used an AMAXA Nucleofector (Lonza, Basel, Switzerland) to nucleofect siRNAs into 10^6 cells using two rounds of nucleofection, 2 days apart. After the second nucleofection, cells were seeded into a 12-well

or Transwell plate (see below) at a density of 1.2×10^5 cells per well to be fully confluent at assay 48 h later. The siRNAs were custom synthesised by Eurofins Genomics (Ebersberg, Germany). The target sequences are: si-Luciferase (ctl), 5′-CGUACGCGGAAUACUUCGA-3′; si-RGS4 (pool of two oligonucleotides, 250 pmol each), 5′-CCUCAAGUCUCGAUUCUAU and 5′-GAAGGAGCCAAGAGUUCA-3′; si-MYRIP (pool of two oligonucleotides, 250 pmol each): 5′-GAUGAGAUGGGCUCCGAUA-3′ and 5′-GAUAUUGAGAGCCGGAUUU-3′; si-GRK2 (pool of two oligonucleotides, 150 pmol each): 5′-UGUCCAGUAACUUGAUUCC-3′ and 5′-GCUCGCAUCCCUUCUCGAAUU-3′; si-AP1 (targeting the AP1 subunit AP1M1, 300 pmol), 5′-AAGGCAUCAAGUAUCGGAAGA-3′; and si-VWF (200 pmol): 5′-GGGCUCGAGUGUACCAAAA-3′.

Plasmids

p-MYC-HIS-RGS4 and pMYC-HIS-RGS4(131-205), pCEFL-RGS4, pCEFL-RGS4 N128A were generously gifted by Dr Kirk Druey (National Institutes of Health, National Institute of Allergy and Infectious Diseases, Bethesda, MD). pMYC-HIS-RGS4-K100E was generated from p-MYC-HIS-RGS4 by using the Q5 site directed mutagenesis kit (New England BioLabs, Hertfordshire, UK). LumGFP plasmid is as described in Blum et al. (2000). Plasmids were nucleofected (2 µg or 10 µg for lumGFP) into 10^6 cells, and cells were seeded into 12-well plates or a Transwell plate at a density of 1.2×10^5 cells per well to be fully confluent and assayed 48 h later. When plasmids were nucleofected with siRNAs, they were added at the second round of nucleofection.

VWF secretion assay

Confluent cells were washed in serum-free (SF) medium [M199, 0.1 mg/ml bovine serum albumin (BSA), 10 mM HEPES-NaOH, pH 7.4] and then incubated in SF medium for 1 h at 37°C. The medium was collected in Eppendorf tubes and centrifuged at 16,000 ***g*** for 10 min at 4°C, and the cells were then lysed in 0.5% Triton X-100 in PBS with protease inhibitors (Sigma-Aldrich, UK; cat. #P8340) to determine VWF levels in both samples (releasate and lysate). Brefeldin A (BFA, 5 µM from Sigma) was added to the cells 1 h before the assay and was then present throughout the experiment. For the NO donor experiment, CysNO or control Cys, freshly prepared according to Cook et al. (1996) and Smith et al. (2018), were added to SF medium at the final concentration of 200 µM to treat confluent cells. Medium was collected and cells were lysed, as above, after 1 h incubation at 37°C.

Relative amounts of VWF were determined by sandwich enzyme-linked immunosorbent assay (ELISA) as previously described (Ferraro et al., 2016).

Transwell experiments

Cells were seeded at 1.2×10^5 cells per well onto Transwell devices (cat. #3460 Corning, Flintshire, UK), and assayed for secretion assay 2 days after, by measuring the amount of VWF in both the apical (top well) and basolateral chamber (bottom well).

lumGFP secretion assay

Cells nucleofected with lumGFP plasmid (Blum et al., 2000; Knipe et al., 2010) and seeded on Transwell inserts were analysed 2 days after nucleofection. The lumGFP secretion assay was performed as the VWF secretion assay, as previously described (Lopes da Silva and Cutler, 2016). Relative amounts of GFP were determined by sandwich ELISA using MaxiSorp plates (Thermo Fisher Scientific) coated with sheep anti-GFP (1:50,000, cat. #4745-1051, BioRad, Watford, UK), followed by blocking and incubation with samples. Plates were washed and incubated with rabbit anti-GFP (1:20,000, cat. #A6455, Thermo Fisher Scientific) followed by washing and a final incubation with goat anti-rabbit-IgG conjugated to horseradish peroxidase (HRP) (1:3000, cat.#AB_2307391 Jackson Laboratories). Plates were developed with o-phenylenediamine dihydrochloride and hydrogen peroxide in a citrate phosphate buffer. Absorbance was analysed at 450 nm in a Thermomax microplate reader (Molecular Devices, San Jose, CA) using a kinetic protocol with a reading every 30 s for 30 min. A standard curve was made using lumGFP nucleofected lysates serially diluted. Results are shown as the percentage of secreted GFP from the total GFP (secreted plus lysate) measured in each sample.

RNA extraction, qPCR and RNA-seq

RNA was extracted using the RNeasy kit (Qiagen, Manchester, UK), retrotranscribed into cDNAs by using the SuperScript III first-strand synthesis system (Thermo Fisher Scientific) and amplified using SYBR Green (DyNAmo SYBR Green qPCR Kit, Thermo Fisher Scientific) on a CFX ConnectTM Real-Time PCR Detection System (BioRad, Watford, UK).

RNAseq was performed as described by Lopes-da-Silva et al. (2019). The RNA-seq raw and processed data were deposited on NCBI GEO under accession code GSE151854.

Decellularisation and flow assay

We grew cells in Ibidi µ-slides VI (cat. # IB-80606, Thistle Scientific, Glasgow, UK) until they were fully confluent. We then attached the slide to a pump system (Harvard Apparatus, Holliston, MA) and placed the slide on the stage of a Zeiss Axiovert 100 inverted microscope (Artisan Technology Group, Champaign, IL) maintained at 37°C. The cells were initially superfused with PBS using a constant wall shear stress of 2.5 dynes/cm^2 (0.25 MPa, 1.4 ml/min), that was maintained throughout the experiment. After 1 min the cells were superfused with NH_4OH 50 mM and Triton X-100 0.1% in PBS for 2 min [the decellularisation solution was adapted from Sixma et al., (1987) and Franco-Barraza et al., (2016)], during which we could observe the cells detaching in real time. We then superfused again with PBS, followed by either whole-blood or platelets (10^8/ml) in Tyrode's buffer for 1 min. After a final perfusion with PBS, µ-slides were fixed under reduced flow (0.7 ml/min) with 4% formaldehyde for 5 min. The µ-slides were fixed for a further 5 min under static conditions, washed with PBS and then processed for confocal immunofluorescence.

Blood and platelets

Blood (7 ml) was drawn from local volunteers into citrate tubes and utilised within few hours. The relevant UK research ethics committee approved the work and the participant gave their written informed consent. Platelets were spare pooled platelets from the London transfusion service of the NHS.

Immunofluorescence and confocal microscopy

After fixation of the decellularised matrix, we incubated the slides with 5% BSA diluted in PBS for 30 min. Samples were subsequently incubated with primary antibodies diluted in 1% BSA in PBS for 1 h. Antibodies used were: anti-VWF (1:1000; cat. #A00A2, Agilent DAKO, Stockport, UK), anti-CD41-FITC (1:200; clone 5B12, cat. #FCMAB195F, from Millipore, Dorset, UK). Secondary antibodies were: Alexa Fluor 488- and 564 (Thermo Fisher Scientific)-conjugated anti-mouse- or rabbit-IgG at 1:500 dilution with PBS. Hoechst 33342 (Thermo Fisher Scientific) was used to counterstain nuclei (1: 10,000). Images were acquired using a spinning disc Ultraview Vox confocal microscope (PerkinElmer, Waltham, MA) with a 20× objective and 1.5× tube lens.

Statistical analysis

Statistical analyses were performed using GraphPad Prism software version 7. All graphs are represented as mean±s.d. Statistical significance was assessed using two-tailed unpaired Student's *t*-test or one-way ANOVA.

Acknowledgements

We thank C. Bertoli and M. Lopes Da Silva for reading and editing the manuscript; K. Druey for kindly sharing the RGS4 constructs; C. Mencarelli, F. Ferraro and P. Boulasiki for their technical help.

Competing interests

The authors declare no competing or financial interests.

Author contributions

Conceptualization: D.F.C., F.P.; Methodology: D.F.C., F.P.; Validation: F.P.; Formal analysis: D.F.C., F.P.; Investigation: F.P.; Data curation: F.P.; Writing - original draft: D.F.C., F.P.; Writing - review & editing: D.F.C., F.P.; Visualization: F.P.; Supervision: D.F.C.; Project administration: D.F.C.; Funding acquisition: D.F.C.

Funding
This work was funded by the British Heart Foundation (PG/14/76/31087) and by the UK Medical Research Council (MC_UU_00012/2).

Data availability
The RNA-seq raw and processed data were deposited on NCBI GEO under accession code GSE151854.

Supplementary information
Supplementary information available online at
https://jcs.biologists.org/lookup/doi/10.1242/jcs.247312.supplemental

References

Baruch, D., Denis, C., Marteaux, C., Schoevaert, D., Coulombel, L. and Meyer, D. (1991). Role of von Willebrand factor associated to extracellular matrices in platelet adhesion. *Blood* **77**, 519-527. doi:10.1182/blood.V77.3.519.519

Berman, D. M., Wilkie, T. M. and Gilman, A. G. (1996). GAIP and RGS4 are GTPase-activating proteins for the Gi subfamily of G protein alpha subunits. *Cell* **86**, 445-452. doi:10.1016/S0092-8674(00)80117-8

Bernardo, A., Ball, C., Nolasco, L., Moake, J. F. and Dong, J.-F. (2004). Effects of inflammatory cytokines on the release and cleavage of the endothelial cell-derived ultralarge von Willebrand factor multimers under flow. *Blood* **104**, 100-106. doi:10.1182/blood-2004-01-0107

Bierings, R., Hellen, N., Kiskin, N., Knipe, L., Fonseca, A.-V., Patel, B., Meli, A., Rose, M., Hannah, M. J. and Carter, T. (2012). The interplay between the Rab27A effectors Slp4-a and MyRIP controls hormone-evoked Weibel-Palade body exocytosis. *Blood* **120**, 2757-2767. doi:10.1182/blood-2012-05-429936

Blum, R., Stephens, D. J. and Schulz, I. (2000). Lumenal targeted GFP, used as a marker of soluble cargo, visualises rapid ERGIC to Golgi traffic by a tubulo-vesicular network. *J. Cell Sci.* **113**, 3151-3159.

Cancino, J., Capalbo, A., Di Campli, A., Giannotta, M., Rizzo, R., Jung, J. E., Di Martino, R., Persico, M., Heinklein, P., Sallese, M. et al. (2014). Control systems of membrane transport at the interface between the endoplasmic reticulum and the Golgi. *Dev. Cell* **30**, 280-294. doi:10.1016/j.devcel.2014.06.018

Cook, J. A., Kim, S. Y., Teague, D., Krishna, M. C., Pacelli, R., Mitchell, J. B., Vodovotz, Y., Nims, R. W., Christodoulou, D., Miles, A. M. et al. (1996). Convenient colorimetric and fluorometric assays for S-nitrosothiols. *Anal. Biochem.* **238**, 150-158. doi:10.1006/abio.1996.0268

Ferraro, F., Kriston-Vizi, J., Metcalf, D. J., Martin-Martin, B., Freeman, J., Burden, J. J., Westmoreland, D., Dyer, C. E., Knight, A. E., Ketteler, R. et al. (2014). A two-tier Golgi-based control of organelle size underpins the functional plasticity of endothelial cells. *Dev. Cell* **29**, 292-304. doi:10.1016/j.devcel.2014.03.021

Ferraro, F., Mafalda Lopes Da, S., Grimes, W., Lee, H. K., Ketteler, R., Kriston-Vizi, J. and Cutler, D. F. (2016). Weibel-Palade body size modulates the adhesive activity of its von Willebrand Factor cargo in cultured endothelial cells. *Sci. Rep.* **6**, 32473. doi:10.1038/srep32473

Franco-Barraza, J., Beacham, D. A., Amatangelo, M. D. and Cukierman, E. (2016). Preparation of extracellular matrices produced by cultured and primary fibroblasts. *Curr. Protoc. Cell Biol.* **71**, 10.9.1-10.9.34. doi:10.1002/cpcb.2

Giannotta, M., Ruggiero, C., Grossi, M., Cancino, J., Capitani, M., Pulvirenti, T., Consoli, G. M. L., Geraci, C., Fanelli, F., Luini, A. et al. (2012). The KDEL receptor couples to Galphaq/11 to activate Src kinases and regulate transport through the Golgi. *EMBO J.* **31**, 2869-2881. doi:10.1038/emboj.2012.134

Giblin, J. P., Hewlett, L. J. and Hannah, M. J. (2008). Basal secretion of von Willebrand factor from human endothelial cells. *Blood* **112**, 957-964. doi:10.1182/blood-2007-12-130740

Houdijk, W. P., De Groot, P. G., Nievelstein, P. F., Sakariassen, K. S. and Sixma, J. J. (1986). Subendothelial proteins and platelet adhesion. von Willebrand factor and fibronectin, not thrombospondin, are involved in platelet adhesion to extracellular matrix of human vascular endothelial cells. *Arteriosclerosis* **6**, 24-33. doi:10.1161/01.atv.6.1.24

Hu, R.-G., Sheng, J., Qi, X., Xu, Z., Takahashi, T. T. and Varshavsky, A. (2005). The N-end rule pathway as a nitric oxide sensor controlling the levels of multiple regulators. *Nature* **437**, 981-986. doi:10.1038/nature04027

Iankova, I., Chavey, C., Clapé, C., Colomer, C., Guérineau, N. C., Grillet, N., Brunet, J. F., Annicotte, J.-S. and Fajas, L. (2008). Regulator of G protein signaling-4 controls fatty acid and glucose homeostasis. *Endocrinology* **149**, 5706-5712. doi:10.1210/en.2008-0717

Jaba, I. M., Zhuang, Z. W., Li, N., Jiang, Y., Martin, K. A., Sinusas, A. J., Papademetris, X., Simons, M., Sessa, W. C., Young, L. H. et al. (2013). NO triggers RGS4 degradation to coordinate angiogenesis and cardiomyocyte growth. *J. Clin. Invest.* **123**, 1718-1731. doi:10.1172/JCI65112

Knipe, L., Meli, A., Hewlett, L., Bierings, R., Dempster, J., Skehel, P., Hannah, M. J. and Carter, T. (2010). A revised model for the secretion of tPA and cytokines from cultured endothelial cells. *Blood* **116**, 2183-2191. doi:10.1182/blood-2010-03-276170

Lopes Da Silva, M. and Cutler, D. F. (2016). von Willebrand factor multimerization and the polarity of secretory pathways in endothelial cells. *Blood* **128**, 277-285. doi:10.1182/blood-2015-10-677054

Lopes-Da-Silva, M., Mccormack, J. J., Burden, J. J., Harrison-Lavoie, K. J., Ferraro, F. and Cutler, D. F. (2019). A GBF1-dependent mechanism for environmentally responsive regulation of ER-Golgi transport. *Dev. Cell* **49**, 786-801.e6. doi:10.1016/j.devcel.2019.04.006

Lui-Roberts, W. W. Y., Collinson, L. M., Hewlett, L. J., Michaux, G. and Cutler, D. F. (2005). An AP-1/clathrin coat plays a novel and essential role in forming the Weibel-Palade bodies of endothelial cells. *J. Cell Biol.* **170**, 627-636. doi:10.1083/jcb.200503054

Mellion, B. T., Ignarro, L. J., Ohlstein, E. H., Pontecorvo, E. G., Hyman, A. L., and Kadowitz, P. J. (1981). Evidence for the inhibitory role of guanosine 3′, 5′-monophosphate in ADP-induced human platelet aggregation in the presence of nitric oxide and related vasodilators. *Blood* **57**, 946-955. doi:10.1182/blood.V57.5.946.946

Nightingale, T. D., Pattni, K., Hume, A. N., Seabra, M. C. and Cutler, D. F. (2009). Rab27a and MyRIP regulate the amount and multimeric state of VWF released from endothelial cells. *Blood* **113**, 5010-5018. doi:10.1182/blood-2008-09-181206

Radomski, M. W., Palmer, R. M., and Moncada, S. (1990). An L-arginine/nitric oxide pathway present in human platelets regulates aggregation. *Proc. Natl. Acad. Sci. USA* **87**, 5193-5197. doi:10.1073/pnas.87.13.5193

Ruiz De Azua, I., Scarselli, M., Rosemond, E., Gautam, D., Jou, W., Gavrilova, O., Ebert, P. J., Levitt, P. and Wess, J. (2010). RGS4 is a negative regulator of insulin release from pancreatic beta-cells in vitro and in vivo. *Proc. Natl. Acad. Sci. USA* **107**, 7999-8004. doi:10.1073/pnas.1003655107

Sixma, J. J., Nievelstein, P. F., Zwaginga, J.-J. and De Groot, P. G. (1987). Adhesion of blood platelets to the extracellular matrix of cultured human endothelial cells. *Ann. N. Y. Acad. Sci.* **516**, 39-51. doi:10.1111/j.1749-6632.1987.tb33028.x

Smith, J. G., Aldous, S. G., Andreassi, C., Cuda, G., Gaspari, M. and Riccio, A. (2018). Proteomic analysis of S-nitrosylated nuclear proteins in rat cortical neurons. *Sci. Signal.* **11**, eaar3396. doi:10.1126/scisignal.aar3396

Stel, H. V., Sakariassen, K. S., De Groot, P. G., Van Mourik, J. A. and Sixma, J. J. (1985). Von Willebrand factor in the vessel wall mediates platelet adherence. *Blood* **65**, 85-90. doi:10.1182/blood.V65.1.85.85

Stevenson, N. L., Martin-Martin, B., Freeman, J., Kriston-Vizi, J., Ketteler, R. and Cutler, D. F. (2014). G protein-coupled receptor kinase 2 moderates recruitment of THP-1 cells to the endothelium by limiting histamine-invoked Weibel-Palade body exocytosis. *J. Thromb. Haemost.* **12**, 261-272. doi:10.1111/jth.12470

Sullivan, B. M., Harrison-Lavoie, K. J., Marshansky, V., Lin, H. Y., Kehrl, J. H., Ausiello, D. A., Brown, D. and Druey, K. M. (2000). RGS4 and RGS2 bind coatomer and inhibit COPI association with Golgi membranes and intracellular transport. *Mol. Biol. Cell* **11**, 3155-3168. doi:10.1091/mbc.11.9.3155

Van Der Poll, T., Van Deventer, S. J. H., Pasterkamp, G., Van Mourik, J. A., Büller, H. R. and Ten Cate, J. W. (1992). Tumor necrosis factor induces von Willebrand factor release in healthy humans. *Thromb. Haemost.* **67**, 623-626. doi:10.1055/s-0038-1648512

Watson, N., Linder, M. E., Druey, K. M., Kehrl, J. H. and Blumer, K. J. (1996). RGS family members: GTPase-activating proteins for heterotrimeric G-protein alpha-subunits. *Nature* **383**, 172-175. doi:10.1038/383172a0

Table S1. List of up- and down-regulated genes in cells untreated (mock) or treated with siRNA against VWF (si-VWF), as measured by RNAseq. Statistical significance was tested by ANOVA. p-values and fold changes are shown.

Click here to Download Table S1

Table S2. List of up- and down-regulated genes in cells untreated (ctl) or treated with TNFalpha as measured by RNAseq. Statistical significance was tested by ANOVA. p-values and fold changes are shown.

Click here to Download Table S2

Table S3. List of up and down-regulated genes in cells grown in M199 compared to EBM2 medium as measured by RNAseq. Statistical significance was tested by ANOVA. p-values and fold changes are shown.

Click here to Download Table S3